

Scanning-Tunneling-Microscopy Study of the Si(111)- 7×7 Rest-Atom Layer Following Adatom Removal by Reaction with Cl

J. S. Villarrubia and John J. Boland

IBM Research Division, Thomas J. Watson Research Center, Yorktown Heights, New York 10598

(Received 2 December 1988)

In this scanning-tunneling-microscopy study we find that the reaction of Cl with Si(111)- 7×7 results in extensive surface modification. On a Cl-saturated and annealed surface, most of the adatom layer is stripped away, permitting the complete underlying Si-rest-atom layer to be imaged for the first time. The structure of this layer is shown to correspond closely to that predicted by the dimer-adatom-stacking-fault model. We directly observe the presence of the stacking fault, an electronic effect associated with this fault, and different outward surface-normal relaxations in the faulted and unfaulted regions of the cell.

PACS numbers: 61.16.Di, 68.35.Bs, 73.20.At, 82.65.My

The structure of the 7×7 reconstructed Si(111) surface has been a long-standing problem in surface science.¹ The presence of dangling bonds (DB's) on the surface represents a significant contribution to the total surface energy and the reduction in the number of these bonds is a major impetus for the reconstruction. The dimer-adatom-stacking-fault (DAS) model of Takayanagi *et al.*² has gained widespread acceptance. Vanderbilt³ suggests that the choice of the 7×7 reconstruction rather than 5×5 or 9×9 is determined by a competition in the rest-atom layer (the layer beneath the outermost one). Energy is saved by the formation of dimer-row domain walls and the concomitant reduction in the number of DB's. However, corner holes where domain walls cross are energetically costly, limiting the number of such walls. In this scheme the outermost (adatom) layer, which is responsible for the now famous scanning-tunneling-microscopy (STM) images of this surface, plays only an incidental role in determining the surface periodicity. To date, the complete underlying rest-atom layer which contains the dimer-row domain walls has never been observed.

In this Letter we present an STM study of the reaction of Cl with the Si(111)- 7×7 surface. The reactivity of Cl and its ability to tie up DB's allows the surface to adopt structures which would otherwise be energetically unfavorable. On a Cl-saturated and annealed surface most of the adatom layer is stripped away, permitting us to image and study the complete underlying Si rest-atom layer for the first time. There are 7×7 domains within this layer which are adjacent to domains that have reverted to a 1×1 unreconstructed surface. The juxtaposition of these reconstructed and unreconstructed domains allows us to directly confirm the presence of the stacking fault on the 7×7 surface. We also observe electronic and relaxation differences between faulted and unfaulted parts of the rest-atom area. The geometry of the 7×7 domains in this layer corresponds closely to that predicted by the DAS model.

This work was performed using an STM similar to that described by Demuth *et al.*⁴ which was mounted in an ion-pumped UHV chamber with a base pressure of $\sim 1\times 10^{-10}$ Torr. The 7×7 surface was generated by heating a phosphorous-doped ($1\ \Omega\text{ cm}$) Si(111) wafer to 1050°C for 30 s. The Cl source was a AgCl electrochemical cell.⁵

Data presented here are of three types; standard STM topographs taken in the constant-current mode, current-voltage characteristics (I - V 's) performed using the sample-and-hole technique developed by Feenstra, Stroscio, and Fein,⁶ and local barrier-height images obtained by applying a 1-kHz 10-mV ($\sim 0.15\ \text{\AA}$) dither to the z piezo (the z direction is perpendicular to the surface) in order to measure dI/dz using a lock-in amplifier. Atom-resolved local barrier-height images have been reported for one other system.⁷ We will use one such image here (Fig. 3) because it has better lateral resolution and lower noise than our topographs of that area. Biases to which we will refer are voltages on the sample with the tip at ground. Hence, at positive bias electrons tunnel from the tip into empty states of the sample. Images displayed here are uncorrected for thermal drift.

Within the DAS model the 7×7 surface consists of a two-layer reconstruction in which the rest-atom double layer (shown in Fig. 1) is capped by an adatom layer (not shown). The rest-atom layer consists of triangular subunits with a 1×1 structure which are either faulted or unfaulted with respect to the bulk layer beneath. These subunits are bounded by dimer-row domain walls which intersect to produce holes at the corners of the cell. The adatom layer consists of six adatoms arranged locally in a 2×2 structure above the shallow hollows within each triangular subunit.

To characterize the Cl-Si interaction we first studied the adsorption at coverages below saturation. I - V curves recorded at unreacted surface sites show peaks arising from the adatom-DB states characteristic of the clean surface.^{8,9} Over reacted sites the corresponding peaks

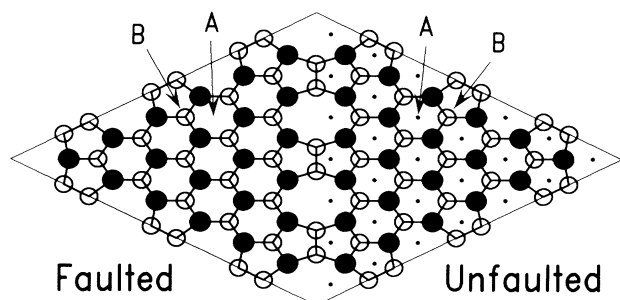


FIG. 1. Schematic of the DAS rest-atom double layer showing deep (A) and shallow (B) threefold hollows. The large filled and open circles represent, respectively, the upper and lower atoms (vertical separation 0.8 \AA) in the double layer. Dots represent the atoms visible in the layer beneath the double layer. The adatom layer (not shown) consists of a 2×2 structure centered on the shallow hollows.

are almost entirely absent and the I - V 's are similar to those observed by Wolkow and Avouris⁹ for NH_3 -reacted sites. The absence of the DB state is reflected in topographs taken below 1.5-V sample bias. At these biases reacted sites appear darker (the tip moves towards the surface) than unreacted ones. In this low-coverage regime, Cl atoms, having reacted via the adatom DB states, occupy on-top sites. Therefore, STM images of the reacted surface retain the 7×7 structure irrespective of whether we image Si or Cl states over reacted sites. In topographs taken above 2 V, reacted sites appear brighter than unreacted ones. We believe that tunneling at these biases is into the tail of the Cl-derived σ^* state which disperses in a band which extends from about 2.4 to 6 eV above the Fermi level and may be further broadened due to hybridization with bulk states.¹⁰

The surface was saturated with Cl and annealed at 470°C for two minutes. After the anneal the only Cl species on the surface is one in which a single Cl atom is bonded in an on-top configuration to each surface Si atom.¹¹ Subsequent I - V curves showed no dangling-bond states or other sharp features, indicating that the surface remained saturated with Cl. Because of the absence of states at low energy, biases of 2 V or higher were used to avoid contact of the tip with the surface.

The 3D rendered topograph shown in Fig. 2 is typical of the surface after a saturation-exposure and anneal cycle. While substantial restructuring has occurred, the saturated surface is manifestly still of 7×7 periodicity. The area of Fig. 2 consists of triangular units bounded by the same crisscross pattern of dimer-row domain walls and corner holes that are observed on the unreacted surface. On that surface, however, the triangular regions would contain six adatoms. A few white protrusions near corner holes are visible in the figure and extend about 2 \AA above the surface. These are the remaining corner adatoms. The rest of the corner adatoms and all of the center adatoms (in this area—other areas re-

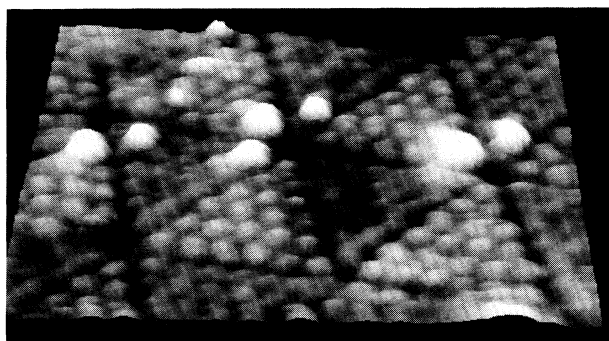


FIG. 2. A topograph of the surface taken after a saturation-exposure and anneal cycle. The large protrusions near the corner holes are the only remaining adatoms. The $88 \times 96\text{-\AA}^2$ area was recorded at 3 V with 0.35-nA tunneling current.

tain some center adatoms as well) have been removed by the Cl.

The structure below the adatom layer in the triangular subunits of Fig. 2 should correspond to the rest-atom layer of the reconstructed surface. In Fig. 3, a barrier-height image from an area adjoining a 7×7 area like the one in Fig. 2, the atoms within one of these triangular

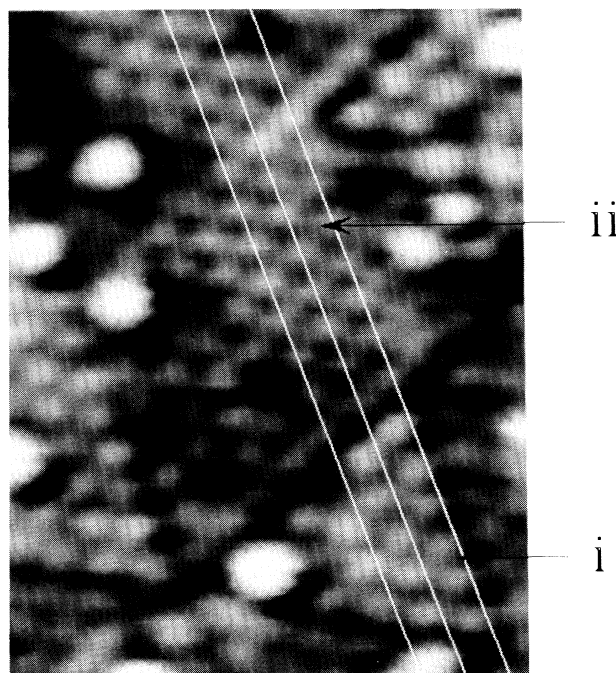


FIG. 3. A local barrier-height (dI/dz) image taken after saturation Cl exposure and annealing, showing the stacking fault. The area is $98 \times 57 \text{ \AA}^2$ and was taken with tunneling stabilized at 0.5 nA and 3 V. The arrows point to areas discussed in the text.

subunits are well resolved, facilitating comparison with the DAS model of this layer's structure. Region i of this image consists of 21 atoms close packed in rows of 6, then 5, then 4, etc., to form an equilateral triangle. The atoms are 3.7 Å apart, in good agreement with the near-neighbor distance in (111) planes of bulk Si. This structure corresponds to the structure of the triangular subunits of the DAS rest-atom layer (Fig. 1). Clearly, region i is half of a 7×7 unit cell from which 5 of the 6 adatoms have been removed.

With the adatom layer removed it is now possible to directly study the rest-atom layer. Region ii of Fig. 3, like region i, is a close-packed layer. In the DAS model, triangular halves of the 7×7 unit cell are referred to as either "unfaulted" or "faulted" depending upon whether their registry with the layer beneath is bulklike or shifted with respect to the bulk positions. Thus, we expect the line separating region i from ii to separate faulted and unfaulted regions, an expectation that is confirmed by extending into region i the lines ruled along rows of atoms in region ii. These are the lines shown in Fig. 3. The rows of atoms in region i fall between, not along, these lines.

Region ii extends for nearly 100 Å (not all shown in Fig. 3) above region i. The size of this domain leads us to assign it as unfaulted, and region i as faulted. Region ii is thus a large domain of bulk-terminated, unreconstructed Si(111). To date, 6 of the 42 rest atoms in each unit cell could be imaged through the adatom layer,^{8,9,12} and the locations of the others were inferred from the positions of the adatoms. Figures 2 and 3 are the first images, however, to show so substantial a portion of the rest-atom layer, and the first to show an extended bulk-terminated domain with which to observe the registry of an adjacent 7×7 cell. As such, it is the most direct confirmation of the stacking fault on this surface.

Note in Fig. 3 that the atoms in the faulted region i are round and distinct, while the pattern in the unfaulted domain has a waffle-iron appearance. This waffle-iron structure was characteristic of unfaulted domains wherever they occurred, whether in the form of unreconstructed 1×1 domains or the unfaulted subunits of 7×7 cells. A 3D rendering of this waffle-iron pattern is shown in Fig. 4(a), where it is apparent that the structure in this image results from the existence of two kinds of threefold hollows. Half of the hollows in Fig. 3, region ii, are dark, corresponding to the deep hollows of Fig. 4(a). The other half are nearly as bright as the maxima, corresponding to the shallow hollows of Fig. 4(a). This pattern matches the model of the Si(111) rest-atom double layer (Fig. 1) in which there are maxima corresponding to the outer atoms, shallow hollows where the lower atoms reside, and deep hollows which penetrate to the next double layer. Thus, in the unfaulted regions, all the atoms of the rest-atom layer are imaged.

However, in the faulted regions only the top atoms in the double layer are imaged. This can be seen in the 3D

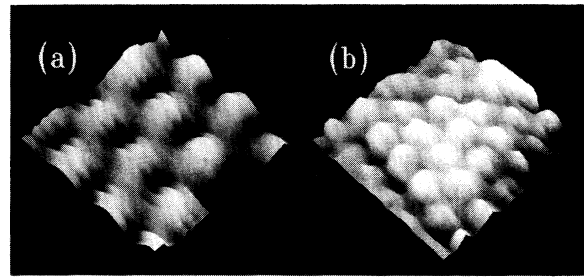


FIG. 4. A comparison of (a) unfaulted and (b) faulted regions of the Cl-passivated rest-atom layer, showing both shallow and deep hollows in the unfaulted, but not in the faulted region. The images are 3D renderings of topographs taken at 2-V sample bias. The subatomic ripples in (a) are noise.

rendering of Fig. 4(b) where the atoms appear round and well separated because the threefold hollows are all comparably deep. As Fig. 1 shows, inequivalent hollows should also exist in faulted regions. Why the different appearance with no significant difference in the geometry of the outermost layer? The presence of Cl on the surface does not cause this difference since *both* types of domains are Cl terminated. The extra intensity in Fig. 4(a) is localized in the region where bonds connect Si atoms in the upper and lower halves of the double layer. We believe the extra intensity is due to an electronic difference in these bonds, which in faulted domains eclipse their counterparts in the double layer beneath (unlike the unfaulted domains, where they are staggered). A state has been observed, nominally at 1.3 eV but with small energy differences between the faulted and unfaulted sides, in $I-V$'s on clean Si.⁸ Like the state which produces the additional intensity in Fig. 4, this state is above the Fermi level and produces more current in the unfaulted domains than in the faulted ones. It is localized in the hollows between the adatoms, where the rest-atom layer is visible. We believe this state is associated with the Si-Si bonds in the rest layer and is, apart from a perturbation due to replacing adatom termination with Cl termination, the state responsible for the additional intensity we see in the shallow hollows in unfaulted regions.

There is yet another difference between the faulted and unfaulted domains. In topographs of the two (see Fig. 2), the fault domains are 0.2 Å higher than the unfaulted ones. Since the only electronic state to exhibit an asymmetry at positive bias is the previously mentioned state at 1.3 eV and since this asymmetry would produce a height difference of the opposite sign, it is likely that this difference is due to geometry, not to an electronic effect. We believe the height difference reflects an enhanced outward surface-normal relaxation in the faulted domains due to the steric interaction between the Si-Si bonds in the rest layer and the eclipsed bonds in the layer beneath. The relaxation has the same sign, but

greater magnitude, than that recently inferred from dynamical LEED analysis of the unreacted surface¹³ and is consistent with an observed base-height difference in STM images of that surface.¹⁴

In this Letter, we have presented an STM study of the Si(111)-7×7 rest-atom layer, the formation of which is the basis for the reconstruction. This was accomplished by reacting the Si(111)-7×7 surface with Cl which stripped off the outermost adatom layer permitting the first images of the complete underlying rest-atom layer. The structure of this layer was observed to correspond closely to that predicted by the DAS model. Parts of this layer, passivated by Cl, have reverted to unreconstructed domains permitting the direct observation of the misalignment of faulted portions of the 7×7 cell. STM images of the rest-atom layer show both electronic and structural differences between the faulted and unfaulted subunits of the cell.

The variety of phenomena occurring in the interaction of Cl and Si, and presumably also with other halogens on Si, promises to be a fruitful area for future investigations. The STM, with its ability to obtain electronic and barrier-height information as well as atomic resolution topography, should make important contributions to our understanding of these systems.

The authors would like to thank N. S. Caswell, Ph. Avouris, F. J. Himpsel, and S. Depp for their comments and review of this manuscript.

¹R. E. Schlier and H. E. Farnsworth, *J. Chem. Phys.* **30**, 917 (1959).

²K. Takayanagi, Y. Tanishiro, S. Takahashi, and M. Takahashi, *Surf. Sci.* **164**, 367 (1985).

³D. Vanderbilt, *Phys. Rev. B* **36**, 6209 (1987).

⁴J. E. Demuth, R. J. Hamers, R. M. Tromp, and M. E. Welland, *J. Vac. Sci. Technol. A* **4**, 1320 (1986).

⁵R. D. Schnell, D. Rieger, A. Bogen, K. Wandelt, and W. Steinmann, *Solid State Commun.* **53**, 205 (1985).

⁶R. M. Feenstra, J. A. Stroscio, and A. P. Fein, *Surf. Sci.* **181**, 295 (1986).

⁷B. Marchon, P. Bernhardt, M. E. Bussell, G. A. Somorjai, M. Salmeron, and W. Siekhaus, *Phys. Rev. Lett.* **60**, 1166 (1988).

⁸R. J. Hamers, R. M. Tromp, and J. E. Demuth, *Phys. Rev. Lett.* **56**, 1972 (1986).

⁹R. Wolkow and Ph. Avouris, *Phys. Rev. Lett.* **60**, 1049 (1988).

¹⁰M. Schlüter and M. L. Cohen, *Phys. Rev. B* **17**, 716 (1978).

¹¹R. D. Schnell, D. Rieger, A. Bogen, F. J. Himpsel, K. Wandelt, and W. Steinmann, *Phys. Rev. B* **32**, 8057 (1985).

¹²Ph. Avouris and R. Wolkow, *Phys. Rev. B* **39**, 5901 (1989).

¹³S. Y. Tong, H. Huang, C. M. Wei, W. E. Packard, F. K. Men, G. Glander, and M. B. Webb, *J. Vac. Sci. Technol. A* **6**, 615 (1988).

¹⁴R. S. Becker, J. A. Golovechenko, E. G. McRae, and B. S. Swartzentruber, *Phys. Rev. Lett.* **55**, 2028 (1985).

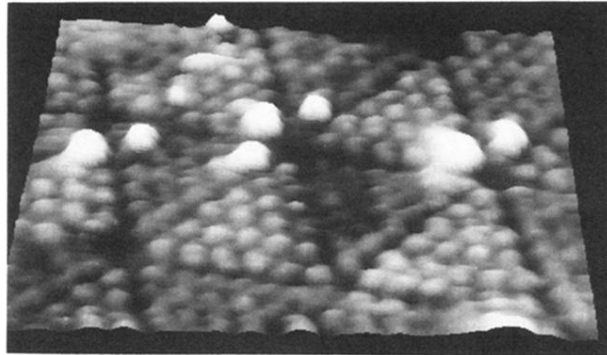


FIG. 2. A topograph of the surface taken after a saturation-exposure and anneal cycle. The large protrusions near the corner holes are the only remaining adatoms. The $88 \times 96 \text{-}\text{\AA}^2$ area was recorded at 3 V with 0.35-nA tunneling current.

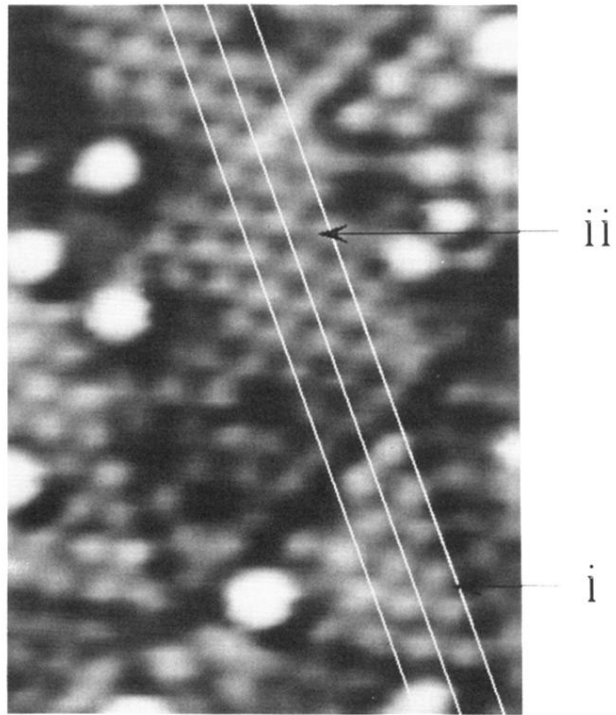


FIG. 3. A local barrier-height (dI/dz) image taken after saturation Cl exposure and annealing, showing the stacking fault. The area is $98 \times 57 \text{ \AA}^2$ and was taken with tunneling stabilized at 0.5 nA and 3 V. The arrows point to areas discussed in the text.

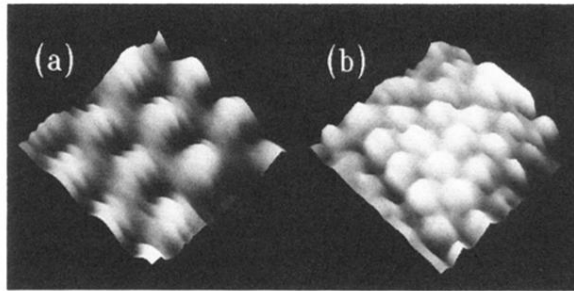


FIG. 4. A comparison of (a) unfaulted and (b) faulted regions of the Cl-passivated rest-atom layer, showing both shallow and deep hollows in the unfaulted, but not in the faulted region. The images are 3D renderings of topographs taken at 2-V sample bias. The subatomic ripples in (a) are noise.